Effect of Solubility and Nucleating Duality of *N,N′*-Dicyclohexyl-2,6-naphthalenedicarboxamide on the Supermolecular Structure of Isotactic Polypropylene

József Varga and Alfréd Menyhárd*

Department of Plastics and Rubber Technology, Budapest University of Technology and Economics, P.O. Box 91, H-1521 Budapest, Hungary

Received December 8, 2006; Revised Manuscript Received February 2, 2007

ABSTRACT: *N,N′*-Dicyclohexyl-2,6-naphthalenedicarboxamide (NJS) is an efficient nucleating agent to prepare isotactic polypropylene (iPP) samples rich in the β-modification (β-iPP). However, NJS is not a selective β-nucleating agent, as the related samples always contain both α and β modification of iPP. Depending on the final temperature of heating (T_f), NJS may be partially or completely dissolved in the iPP melt. The dual nucleation ability of NJS was studied by polarized light microscopy (PLM) and calorimetry (DSC). It was established that the lateral surface of the needle crystals of NJS acts as α-nucleating agent. Because of the solubility and dual nucleating ability of NJS, a wide variety of supermolecular structures may form in its presence. The feature of the structure formed during the crystallization of iPP depends on the concentration of the nucleating agent, on the end temperature of heating, and on the thermal conditions during cooling and crystallization. In this study we observed an $\alpha\beta$-transcrystalline layer development on the lateral surface of the needle crystals of NJS, dendritic and microcrystalline structures, and a spectacular "flower"-like agglomerate of β- and α-crystallites. A model was proposed to explain the dual nucleating effect of NJS.

Introduction

In the past two decades numerous research groups dedicated considerable attention to the preparation of the β-modification of isotactic polypropylene (β-iPP) under laboratory and industrial conditions. The crystalline structure, melting, and crystallization characteristics as well as properties of β-iPP formed were extensively studied (see refs 1 and 2 and references therein). The toughness (ductility) and impact resistance of β-iPP are superior to those of the traditional α-form of iPP (α-iPP).[1,2] These characteristics of β-iPP, which are very advantageous in several applications, justify the extensive basic and applied research related to this material.

Under practical conditions β-iPP can be produced with the help of efficient, selective β-nucleating agents. An overview about the available β-nucleating agents was published recently.[1] The selectivity of β-nucleating agents is characterized by the polymorphic composition of the polymer, which is expressed quantitatively by the *k* value derived from X-ray diffraction measurements[3] or by the area of the melting peak of the β-modification determined by calorimetry.[4] The efficiency of nucleating agents is usually evaluated by calorimetry. The increasing rate of crystallization and higher peak temperature of crystallization determined at a constant cooling rate indicate larger efficiency.[4]

The first efficient β-nucleating agent was the γ-form of linear *trans*-quinacridone introduced by Leugering.[5] The efficiency of a two-component β-nucleating agent consisting of pimelic acid and calcium stearate was demonstrated by Shi et al.[6] Similarly efficient compounds, which have more defined composition and structure, are the calcium salts of pimelic and suberic acid produced in our laboratory.[7,8]

N,N′-Dicyclohexyl-2,6-naphthalenedicarboxamide is also an efficient β-nucleating agent, which was developed and marketed in the past few years.[9] This nucleating agent is sold under the trade name of NJ Star NU 100, and it is available for scientists only through industrial contacts. This nucleator is designated as NJS in this paper. The nucleation efficiency of NJS was proved by X-ray diffraction measurements and detailed calorimetric studies.[4,9−18] NJS proved to be an efficient nucleating agent also in production under industrial conditions. The β-phase content, or *k* value, of compression-molded,[16,17] extruded,[18] and injection-molded[19−26] parts produced with NJS is relatively high. The mechanical and other properties of the processed parts were determined as well. The results of mechanical measurements and fracture mechanics studies done on PP samples nucleated with NJS confirmed the previous observations about the advantageous properties of β-iPP.[1,2] The discussion of the results of these studies is out of the scope of this work; a more detailed analysis can be found in the chapter of Grein.[2] Experimental results achieved under real processing conditions indicated that the NJS concentration should surpass a lower threshold value ($\sim$300 ppm) to get products rich in the β-iPP. Accordingly, certain authors refer to sub- and supercritical concentrations of this nucleating agent.[19,21]

The supermolecular structure of iPP nucleated with NJS was studied mostly by PLM on sections cut from processed samples.[11,22,25] Microcrystalline structure was found in these samples, probably due to the large concentration of the nucleating agent and the high cooling rate prevailing under the processing conditions used. However, unambiguous conclusions about the structure formation cannot be drawn from these studies, since cooling conditions were not controlled sufficiently. It is worth noting that AFM studies of Zhou et al.[27,28] and PLM observations of Behrendt et al.[29] delivered useful information, which helped for a better understanding of the nucleating mechanism of NJS.

Attention should be paid to the fact that the effect of $\beta\alpha$-recrystallization, which seriously complicates the proper determination of polymorphic composition, usually has not been

* To whom correspondence should be addressed: Fax 36-1-463-3474, e-mail amenyhard@mail.bme.hu.

10.1021/ma062815j CCC: $37.00
Published on Web 03/07/2007

eliminated during the calorimetric studies of iPP samples nucleated with NJS. Such recrystallization occurs during the heating of samples previously cooled under the critical $T_R^* = 100$ °C temperature.[1] In microsections, cut from processed samples, the occurrence of $\beta\alpha$-recrystallization cannot be avoided. Thus, a smaller or larger melting peak of the α-iPP can be practically always observed on the melting traces of such samples.[16−26] Consequently, conclusions drawn from calorimetric measurements done on samples cooled below T_R^* must be treated with the utmost caution.[1,4] This note holds for those contributions which consider the melting peaks to estimate the amount of β-phase and its melting temperature. The critical evaluation of these results is again beyond the scope of this article.

In a previous paper we presented a comparative study of various β-nucleating agents.[4] By eliminating the $\beta\alpha$-recrystallization, we have demonstrated that calcium pimelate and suberate have the highest selectivity among all known β-nucleating agents. It was also pinpointed that NJS is not a selective β-nucleating agent, and α-iPP always forms in its presence. This behavior of NJS was termed as dual nucleating ability. The critical concentration observed for this nucleating agent is related to its partial solution in the iPP melt.[4] The subject of this paper is a more detailed study on how the solubility of NJS affects the crystallization, polymorphic composition, and supermolecular structure of iPP. The conclusions are supported by PLM and calorimetric measurements. The observations related to the dual nucleation of NJS are discussed in detail.

Experimental Section

Materials. The Tipplen H 890 grade iPP homopolymer (MFR = 0.35 g/10 min at 230 °C/2.16 kg), used in the study, was supplied by TVK, Hungary. Commercial NJS was added to the polymer in the concentration range (C) from 10 to 1000 ppm. The polymer and the nucleating agent were homogenized in a Brabender W 50 EH internal mixer at 200 °C and 50 rpm for 10 min.

Methods. The structure, crystallization, and melting characteristics of the nucleated samples were studied by polarized light microscopy (PLM) and differential scanning calorimetry (DSC). PLM studies were performed in polarized light using a Leitz Dialux 20 microscope equipped with a Mettler FP82 hot stage. In order to determine of the optical character of the samples studied, a λ plate was located diagonally between the crossed polarizers. The colored PLM micrographs were recorded by a DMC model 1 digital camera and the Image Pro-Plus photo editor software. The samples were crystallized under isothermal or nonisothermal conditions after the elimination of thermal and mechanical history by holding the samples at $T = 200$ °C for 5 min and then cooled to room temperature. Subsequently, the samples were heated up to the final temperature of heating (T_f) somewhere between 180 and 260 °C. At T_f, the time of heat treatment (t_f) was 5 min. The melted samples were cooled from T_f to the crystallization temperature (T_c) at a rate of 5 °C/min or quenched. Samples partially crystallized at a given temperature (T_c) were always heated up from T_c without cooling to lower temperature. In this case, the β-phase melts separately without $\beta\alpha$-recrystallization at about 155 °C.[1] The heating rate was 5 °C/min. Pictures from the residual structure of the partially melted samples were captured. We should emphasize here that the samples were not subjected to temperatures higher than 200 °C before the systematic PLM study in order to minimize of the influence of the partial dissolution of NJS and avoid the thermooxidative degradation of the sample. The crystallization and melting curves were registered by a Perkin-Elmer DSC-7 calorimeter at heating and cooling rate $V_h = V_c = 10$ °C/min after erasing of the thermal history of the samples by heating at $T = 200$ °C for 5 min. During nonisothermal crystallization, the end temperature of cooling was set to $T_R^* = 100$ °C to eliminate the effect of $\beta\alpha$-recrystallization disturbing the determination of polymorphic composition.[1] SEM micrographs were taken from selected samples using JEOL ISM 5600 LV equipment. The surface of the samples was etched with a permanganate solution.[30]

Results and Discussion

Supermolecular Structure of β-Nucleated Samples. The crystallization of samples containing different amounts of nucleating agents was studied under various conditions by PLM. Additional information about the structure formation and structural characteristics of the samples of mixed polymorphic composition was obtained after the separate melting of the β-iPP. Recall that β-iPP melts at lower temperature than α-iPP.[1]

PLM studies proved that NJS dissolves partially or completely in the iPP melt and recrystallizes during cooling. The extent of dissolution, the size of the recrystallized nucleating agent, and the supermolecular structure formed depend on the concentration of the nucleating agent, on the final temperature of heating (T_f), on the cooling conditions, and on the thermal conditions of crystallization. According to our PLM studies, very diverse structures can develop in the presence of NJS. Depending on the combination of the factors listed above, we observed the development of the following characteristic morphologies: (i) formation of a transcrystalline layer on the crystal surface of the nucleating agent, (ii) formation of dendritic structures, (iii) development of microcrystalline agglomerates, and (iv) formation of "flower"-like structure.

In the studied concentration range, the particles of the dispersed nucleating agent cannot be detected by PLM in melt films prepared from the polymer containing NJS. However, at larger nucleating agent concentration (300 ppm and above) and at high final temperature of heating (T_f), the dissolved nucleating agent recrystallizes from the melt in the form of needlelike crystals. Using multiple melting and recrystallization cycles with continuously increasing T_f, we can increase the size of NJS needle crystals (Figure 1a). Transcrystalline structure forms on the surface of the crystals, which helps us to explain several characteristics of the nucleation mechanism of NJS. Mixed polymorphic structure forms on the lateral surface of the needle crystals below the $T(\beta\alpha)$ temperature,[1] while a structure richer in the β-iPP appears around the tip of the needles (Figure 1b,c). These structures can be unambiguously identified by the analysis of the structure left behind by the separate melting of the β-phase (Figure 1c). The birefringence of the β-phase formed on the surface of the needle crystals is strong, indicating (Figure 1b) that the chain-folded lamellae of the β-phase stand on their edge. Consequently, the molecular chains are lying nearly in the plane of the sample.[1] This latter observation agrees well with the AFM studies of Zhou et al.[27,28] PLM micrographs prove that NJS is not a selective β-nucleating agent due to the partial α-nucleating effect of its lateral crystal surface. This α-nucleating effect can be shown also directly. For this purpose the nucleated sample was crystallized above the critical upper temperature of the formation of β-iPP, namely $T(\beta\alpha) = 141$ °C.[1] In this case a transcrystalline layer forms, which consists entirely of the α-iPP (Figure 2). The α-nucleating effect is proved by the fact that nucleus density is much larger on the surface of NJS than in bulk.

The characteristics of the supermolecular structure developing around the needle crystals are demonstrated by the model presented in Figure 3. An α-transcrystalline front develops from the α-nuclei being in abundant large density on the lateral surface of the needles. On the other hand, triangular spherulite slices grow from individual β-nuclei located randomly on the lateral surface of NJS. A straight boundary line forms between

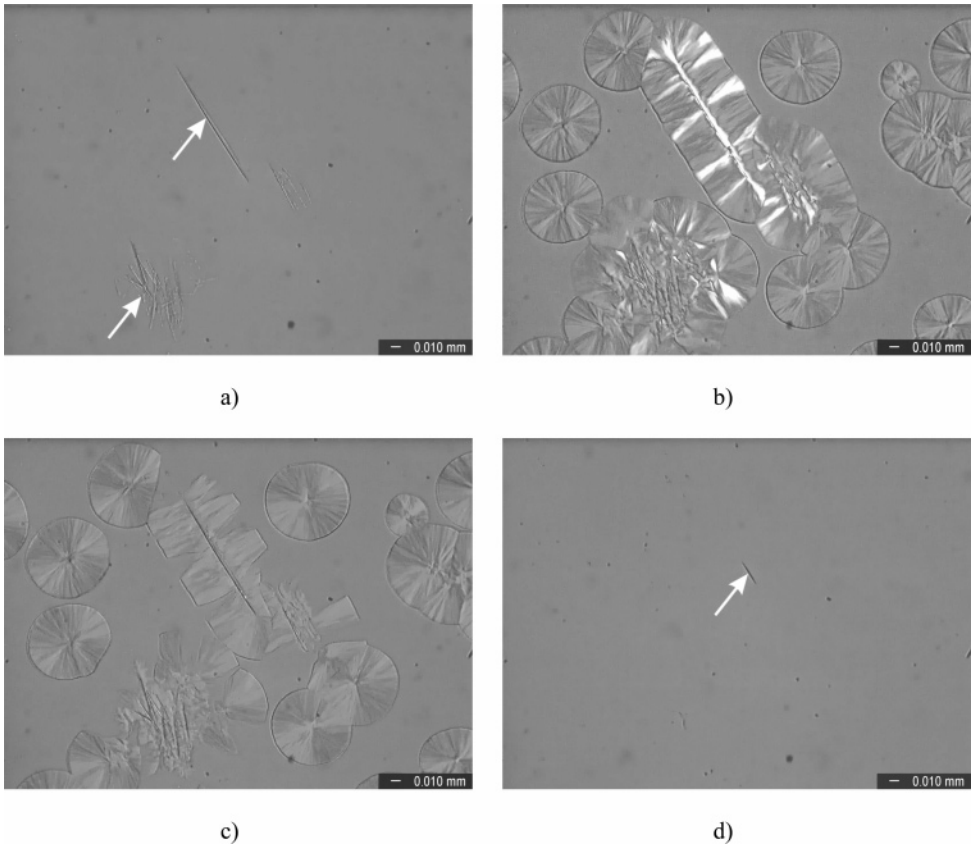

Figure 1. PLM micrographs demonstrating the crystallization of iPP on the surface of NJS needle crystals (C = 500 ppm, T_f = 240 °C, V_c = 5 °C/min, T_c = 135 °C): (a) needle crystal of NJS recrystallized during cooling at T_c = 135 °C; (b) crystallization of iPP at T_c = 135 °C, t_c = 40 min; (c) structure left behind by the separate melting of the β-phase at 156 °C; (d) needle crystal of NJS remaining in the melt at 220 °C.

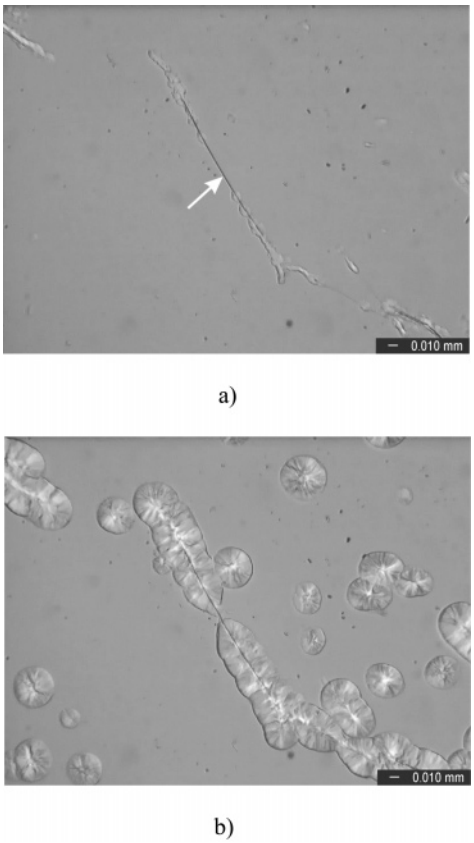

Figure 2. Development of α-transcrystalline structure on the lateral surface of NJS at T_c = 145 °C above the upper limit temperature of the formation of β-iPP ($T(\beta\alpha)$) (C = 500 ppm, T_f = 240 °C, V_c = 5 °C/min): (a) t_c = 30 min, (b) t_c = 105 min.

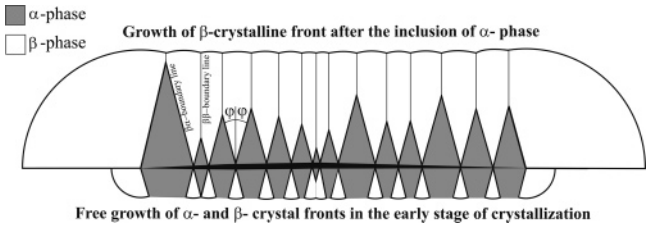

Figure 3. Model for the mechanism of crystal growth on the surface of iPP on the surface of NJS leading to the formation of a mixed polymorphic composition: (a) free growth of the α- and β-crystalline front; (b) free growth of the β-phase after the inclusion of the α-phase.

the α-transcrystalline layer and the β-spherulite slices. In accordance with our earlier quantitative analysis,[31,32] the slope of the straight line (φ) depends on the relative growth rate of the α- and β-phases ($V_r = V_\beta/V_\alpha$):

$$V_r = \frac{1}{\cos \varphi}$$

The initial stage of crystallization on the surface of the nucleating agent, when both the α- and β-crystalline fronts grow unrestricted, is shown in the lower part of Figure 3. Since V_r > 1 in the temperature range between $T(\beta\alpha)$ and $T(\alpha\beta)$,[1,31,33] β-spherulite slices grow faster and thus hinder the expansion of the α-transcrystalline front in the later stages of the crystallization. As a consequence, the α-transcrystalline layer forming on the lateral surface of the needle crystal remains back as an inclusion, as shown by the sketch in the upper part of Figure 3. The formation of the inclusion of α-phase is demonstrated by the PLM micrograph presented in Figure 4. We can clearly recognize that the transcrystalline inclusions of the α-modification (shown by arrow) formed on the surface of

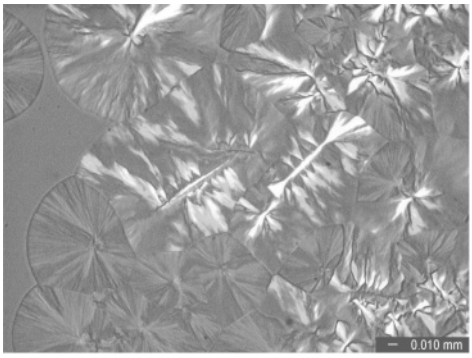

a)

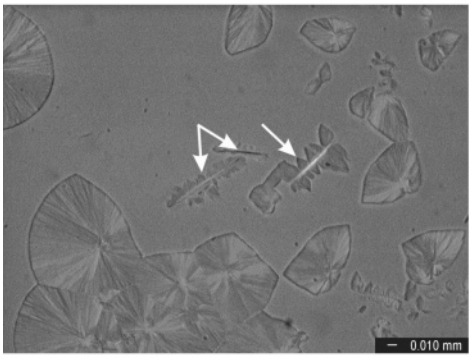

b)

Figure 4. PLM micrographs showing the crystallization of iPP on the surface of NJS needle crystals at T_c = 130 °C (C = 500 ppm, T_f = 240 °C, V_c = 5 °C/min): (a) structure formed after t_c = 20 min; (b) structure left behind after the separate melting of the β-phase at 156 °C.

the nucleating agent are remaining after the separate melting of the β-phase. Assuming as an ideal case that a β-nucleus is located at the tip of the needle, which would induce the formation of a β-spherulite, then the phase structure and the $\beta\alpha$-boundary line would develop according to the scheme shown in Figure 3. This assumption could explain the larger β-phase content in the vicinity of the tip of the needle. However, the slope of the $\beta\alpha$-interface in the PLM micrograph (Figures 1c and 4b) does not agree with that shown in Figure 3. This contradiction probably results from the disturbance caused by the microcrystalline nucleating agent forming around the tip of the needle. We illustrate this effect in a subsequent section.

The relative amount of the β-phase in the mixed polymorphic transcrystalline structure increases with decreasing the temperature of crystallization. The increase of the β-content is caused by the continuous increase of the number of β-nucleating sites formed on the lateral surface of needle crystals and by increase of V_r with decreasing T_c.[1,31,33] Hence, the growth of the α-transcrystalline front stopped earlier and earlier by the β-spherulite slices. This is well discernible after the separate melting of the β-phase in Figure 4b. Larger V_r is indicated by the steeper slope of the interface between the α- and β-phases in the PLM micrographs.

Melting curves of isothermally crystallized samples are shown in Figure 5 as a function of temperature. Samples crystallized above $T(\beta\alpha)$ (T_c = 142 and 145 °C) contain only the α-modification of iPP. The melting curves resemble very much those recorded on samples isothermally crystallized at high temperatures.[34] Note that for samples crystallized at high temperatures the twinning of the melting peak of the α-phase is often related to a modification transition from α_1 to α_2 crystals

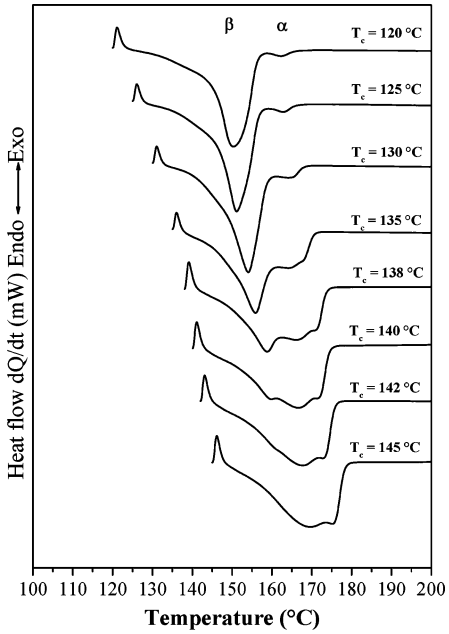

Figure 5. Effect of the temperature of crystallization on the DSC melting traces of β-nucleated iPP samples (C = 1000 ppm, T_f = 220 °C, $T_R = T_c$, V_h = 10 °C/min).

(see ref 33 and references therein). The melting peak of the β-phase superposes onto the two α-peaks in the melting curves of samples crystallized below $T(\beta\alpha)$ (Figure 5, T_c = 135−140 °C). As T_c decreases, the melting peak of the β-phase becomes more and more pronounced in accordance with the explanation given above. If $T_c \leq$ 130 °C, the peak duplication of α-phase does not take place.[34] Consequently, on the melting curves only two peaks appear, indicating the melting of the α- and β-phases. The melting temperature of both the α- and β-phases increases with increasing T_c according to the kinetic theory of crystallization.[33]

A characteristic dendritic structure forms, if samples containing a large amount of nucleating agent (500 and 1000 ppm) are quenched from high T_f (T_f = 260 °C) to the temperature of crystallization (Figure 6). The formation of this structure can be explained by the fact that the crystallization of the nucleating agent is faster than the crystallization of iPP. Dendrites have mixed polymorphic composition proved by the presence of α-crystallites left behind by the separate melting of the β-phase (Figure 6c). Since the nucleating agent crystallizes in the form of very fine needle crystals upon fast cooling, the crystallites of the α-phase of iPP growing on the lateral surface of the needles show a very fine, network-like distribution. If the sample slightly cooled after the separate melting of the β-phase, the further growth of the residual α-crystallites marks this network structure (Figure 6d). It is worth noting that the β-phase grows slightly further during the melting experiment, forming a thin spherulite ring with higher melting temperature. This ring is conserved during cautious melting, and it can serve as marker for the position of the crystalline front (Figure 6d marked by arrow). PLM micrographs prove also that the β-modification, which grows faster than the α-phase, occludes completely the primary α-crystallites as crystallization proceeds. Later, the growing crystalline front contains only the β-phase of iPP. α-Crystallites cannot be detected in the β-phase formed after occlusion. This was proved by the PLM micrograph taken after the separate melting of the β-phase (Figure 6c,d).

At small concentrations, the nucleating agent recrystallizes at lower temperature, at which the rate of crystallization of iPP

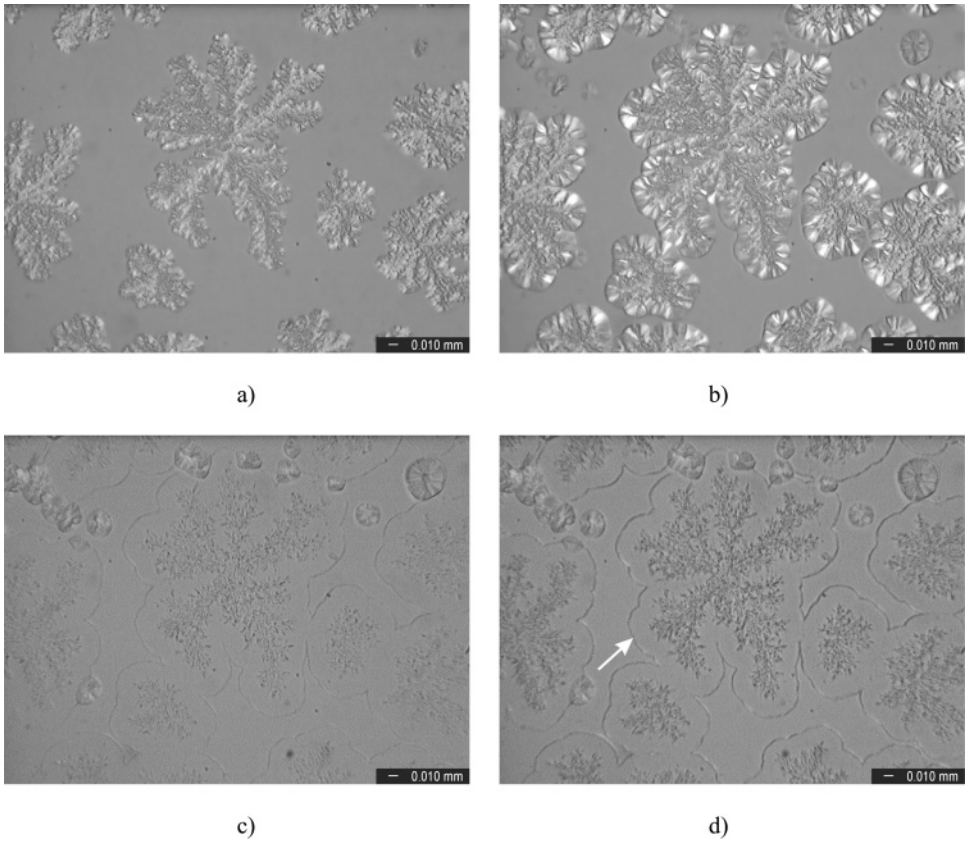

Figure 6. Dendritic crystallization of the β-phase of iPP on the surface of recrystallized NJS at 130 °C (C = 1000 ppm, T_f = 260 °C): (a) crystallization during quenching to T_c = 130 °C; (b) T_c = 130 °C, t_c = 3 min; (c) structure left behind after the separate melting of the β-phase of iPP at T = 154 °C; (d) crystallization of α-iPP induced by microcrystalline α-phase agglomerates during cooling down to about 135 °C.

is comparable to that of the nucleating agent. This results in simultaneous crystallization of the two components, i.e., iPP and NJS. In such cases a mixed polymorphic microcrystalline structure forms, in which crystallites of the α-modification are homogeneously distributed in the β-phase (Figure 7). This morphology is confirmed by the structure left behind by the separate melting of the β-crystals. Figure 7 also shows that the growth rate of the microcrystalline phase is larger than that of the individual α-spherulites formed simultaneously. This statement is supported by the formation of the leaflike α-spherulite inclusion shown in Figure 7. We note here that a similar structure may form also in samples containing simultaneously α- and β-spherulites. Processes leading to the formation of inclusions are analyzed quantitatively in ref 31.

Spectacular structure forms when a sample containing the needle crystals of the nucleating agent is heated to relatively low T_f (220 °C). Under these conditions, the NJS crystals do not dissolve completely in the melt. In subsequent crystallization and melting cycle with lowered T_f (T_f = 180 °C), a "flower"-like structure forms, which consists of a needle crystal of nucleator with transcrystalline overgrown and a microcrystalline agglomerate at its tip (Figure 8). The structure formation around the tip of the nondissolved needle crystal was induced by the recrystallized nucleating agent. This structure has mixed a polymorphic composition similarly to the microcrystalline structure discussed above (Figure 7). The micrographs presented in Figure 8 display that the dissolution of the nucleating agent is a direction-dependent (anisotropic) process; the preferred location of dissolution is the tip of the needle. On the other hand, dissolution does not seem to occur along the lateral surface of the needles (Figure 8b).

At high temperatures mainly α-spherulites form in samples containing small amounts of NJS. Melt inclusions form inside the spherulitic structure at latter stages of crystallization. The concentration of dissolved NJS increases monotonously inside the melt inclusion during iPP crystallization and starts to crystallize upon saturation. As a consequence, mixed polymorphic microcrystalline agglomerates form inside the melt inclusions, similar to those presented in Figure 7. This is shown in Figure 9 by a series of micrographs. SEM micrographs taken from the etched surface of a microcrystalline aggregate indicate the presence of β-lamellae laying flat on and standing edge on (Figure 10a,b) as well.

Relevant information related to the results presented in previous paragraphs was published recently by other groups. Zhou et al.[27,28] showed that NJS crystals grown from solution (and not from iPP melt) induce the epitaxial growth of the β-phase of iPP. Behrendt et al.[29] observed the formation of dendritic structures similar to those shown in Figure 6 during the crystallization of samples heated to high T_f temperatures and containing a large amount of NJS. These authors called already the attention to the partial dissolution of NJS but did not study in detail the crystallization process and its controlling factors. They did not carry out melting experiments either, which could have supplied valuable information about the development of the crystalline structure. In a recent paper by Vychopnova et al.,[35] one can find a PLM micrograph of a microsection cut from a sample crystallized isothermally at 140 °C. The structure resembles the "microcrystalline" agglomerate, or something like that. For the formation of this structure, the authors have given a speculative explanation based on the β- to α-growth transition,[1]

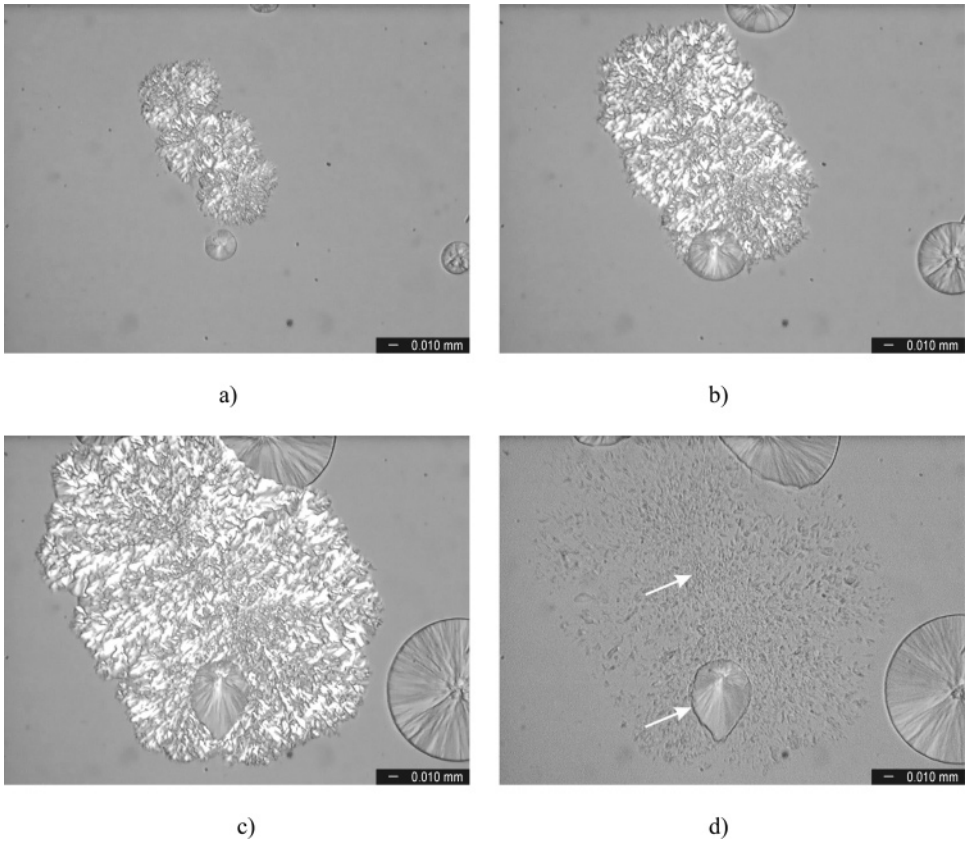

Figure 7. Formation of a microcrystalline agglomerate with mixed polymorphic composition on the surface of recrystallized NJS at $T_c = 135$ °C ($C = 50$ ppm, $T_f = 240$ °C): (a) $t_c = 15$ min, (b) $t_c = 30$ min, (c) $t_c = 60$ min, (d) structure left behind after the separate melting of the β-phase at 154 °C.

which seems to be inconsistent with our experimental observations.

PLM micrographs indicated that the structure developing in the presence of NJS differs significantly from that which occurred in the samples containing calcium pimelate and suberate nucleating agents. In the presence of the later, β-hedrites form in the early stage of the crystallization, which become randomized during their growth and transformed into quasi-spherulites.[1,36,37] The characteristics of the structure induced by NJS are determined by the dual nucleation, i.e., triggering the growth of α- and β-phase simultaneously, and solubility of this nucleating agent, as well as by the thermal conditions during cooling and crystallization.

Effect of the Final Temperature of Heating on the Crystallization and Polymorphic Composition in iPP. Abundant experimental information is available in the open literature about the effect of the final temperature of melting (T_f) on the crystallization of iPP (see ref 31 and references therein). These results suggest that a smaller or larger number of self-nuclei remain in the melt above the melting point of the polymer. These self-nuclei considerably influence the rate of recrystallization after melting and the characteristics of the resulting supermolecular structure. However, a critical T_f^* temperature exists, above which an "empty" melt free of self-nuclei is present. Further increase of the final temperature of heating above this threshold does not influence the recrystallization of the polymer.[31] We must note here that T_f^* depends also on the time of heating and on the supermolecular structure of the initial sample.

The effect of melting conditions on the crystallization and melting behavior of iPP becomes markedly more complicated in the presence of partially soluble nucleating agents, since the amount of dissolved and heterogeneous (nondissolved) nucleating agent depends on T_f. The relations are complicated even more by the fact that the amount of nondissolved, heterogeneous nucleating agent influences also the polymorphic composition of the sample. Recall that the relative fraction of the β-phase depends on the concentration of the nucleating agent.[4] The β-nucleating agents work only if their crystallites are present in the iPP melt. As a consequence, the initial concentration of the nucleating agent, its recrystallization during cooling, and the final temperature of heating all influence the crystallization, the polymorphic composition, and the supermolecular structure of the samples. It has to be emphasized that microcrystalline agglomerates of α-phase form always during the cooling of β-nucleated iPP samples, when T_f is lower than T_f^*.[31,38]

The effect of the factors mentioned above is demonstrated by the calorimetric melting curves in Figure 11a which were recorded on samples crystallized after heating them to systematically increasing T_f temperatures. The melting curve of the sample crystallized after the first heating to 220 °C is inserted at the top of Figure 11a (similarly to Figures 12 and 14). Note that the NJS content of the sample (100 ppm) was smaller than the "critical" value. Nevertheless, a product rich in the β-iPP forms at low T_f values ($T_f \leq 205$ °C). The β-content decreases with increasing T_f, and practically only the α-modification forms at $T_f \geq 220$ °C (Figure 11a). The experimental results, which are in accordance with those obtained by PLM, unambiguously indicate that NJS dissolves in the melt, and the extent of its dissolution increases with T_f, leading to a decrease in efficiency. These results agree well with the observation that the peak temperature as well as the temperature range of crystallization shift toward lower values with increasing T_f (Figure 11b). It should be noticed that after high T_f the crystallization did not finish always during cooling (Figure 11b). In this case, the

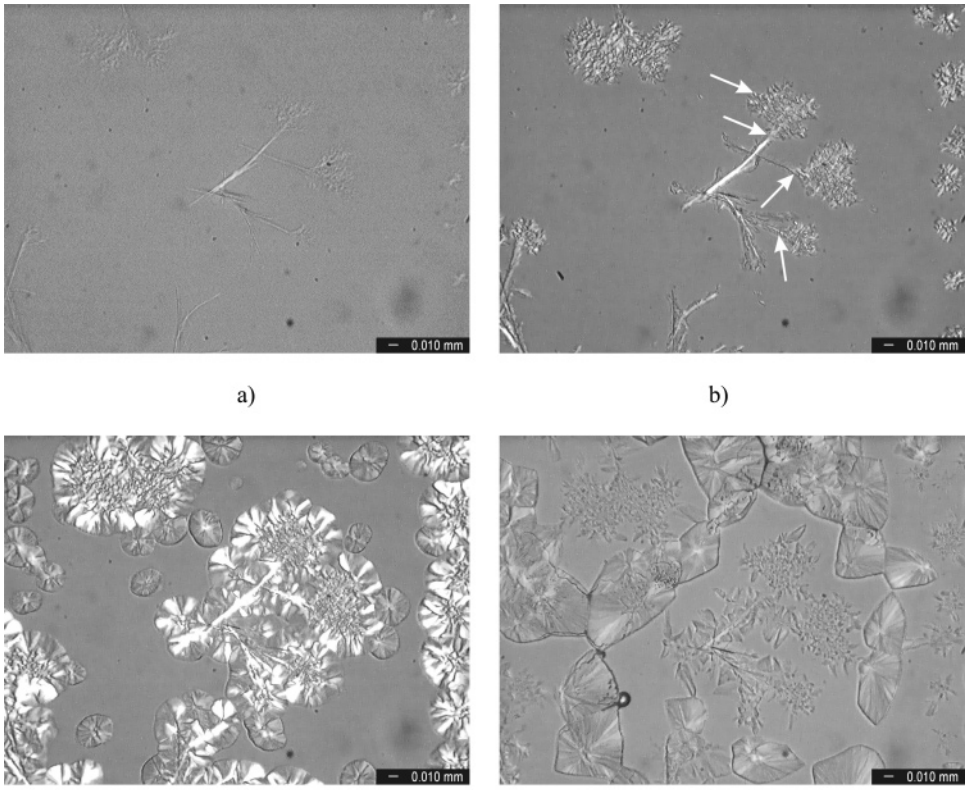

Figure 8. "Flower"-like structure formed in the vicinity of the tip of a NJS needle crystal ($C = 300$ ppm, $T_f = 180$ °C, $T_c = 135$ °C, quenched sample): (a) $t_c = 1$ min, (b) $t_c = 5$ min, (c) $t_c = 20$ min, (d) structure left behind after the separate melting of the α-phase at 156 °C.

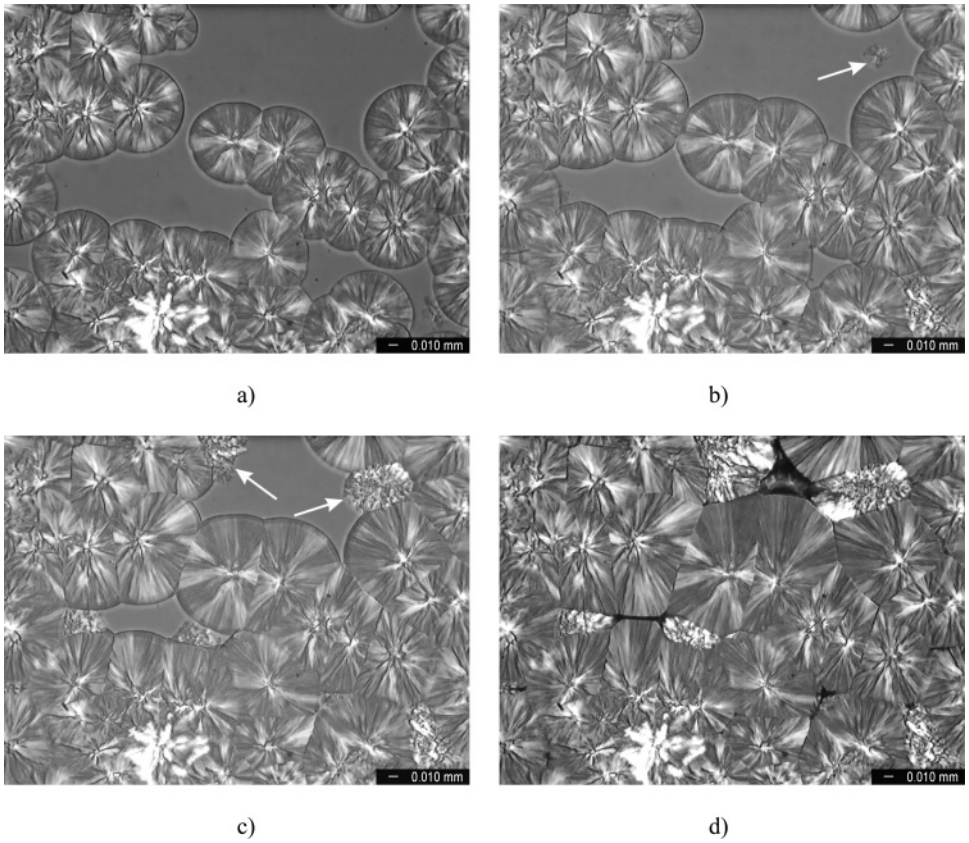

Figure 9. Structure formed on the surface of NJS recrystallized inside a melt inclusion ($C = 50$ ppm, $T_f = 220$ °C, quenched sample, $T_c = 130$ °C): (a) $t_c = 12$, (b) $t_c = 15$, (c) $t_c = 20$, (d) structure after overall crystallization.

samples were kept for 5 min at this temperature for finishing the crystallization. We note here that the increase of the peak temperature of crystallization (T_{cp}) with decreasing T_f cannot be traced to increasing number of self-nuclei of the α-form.

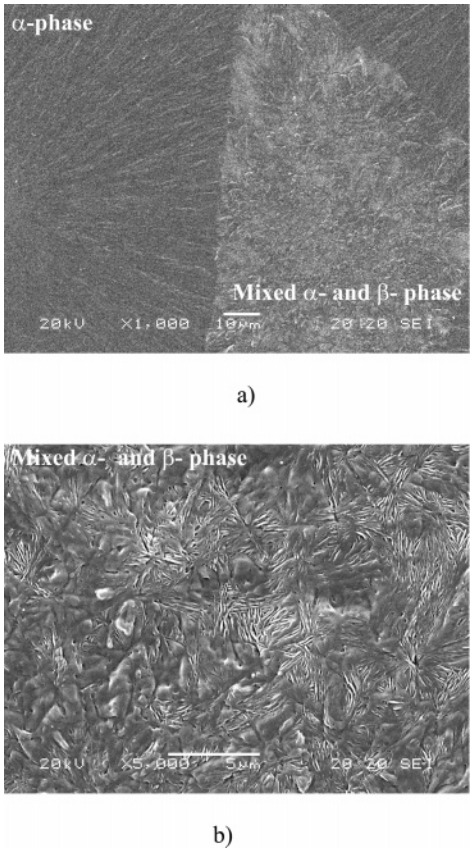

Figure 10. SEM micrograph taken from the etched surface of a film with a mixed αβ-microcrystalline structure formed inside a melt inclusion (C = 50 ppm, T_f = 220 °C, T_c = 130 °C): (a) total area; (b) structure of the mixed α- and β- phase shown at larger magnification.

This would certainly lead to the formation of a structure with increasing α-phase content.[38] The experimental results indicate just the opposite trend (Figure 11a).

According to our results, samples containing mainly β-iPP can be produced also at small NJS content, if T_f is sufficiently low. At 50 ppm nucleating agent content this occurs when $T_f \leq 195$ °C (Figure 12). In Figure 13 we show the dependence of the peak temperature of crystallization on the final temperature of heating at "subcritical" nucleating agent content. The peak temperatures monotonously decreased with increasing T_f at both concentrations of NJS, which is connected with its partial dissolution. The dramatic decrease of T_{cp}, shown by dashed line in Figure 13, seems to indicate the complete dissolution of NJS. The reproducibility of the experiments is excellent, which is proved also by the series of experiments shown in Figure 14. In this series, the T_f has been changed in a systematic way. First we crystallized the sample heated to a higher temperature (T_f = 220 °C), then repeated the process three times with a smaller T_f value, and finally we increased T_f again. It can be claimed that the value of T_f unambiguously governs the polymorphic composition of the sample (Figure 14a) and the crystallization process (Figure 14b).

The "critical" nucleating agent content seems to be a relative quantity, since its numerical value depends on T_f. The optimum amount of nucleating agent must be selected according to the maximum T_f value prevailing during the processing of the polymer. It is also obvious that the higher is the maximum melt temperature reached during processing, the more nucleating agent must be added to iPP in order to prepare a product rich in β-phase content. The observation that the "critical" nucleating agent content necessary for the production of injection-molded

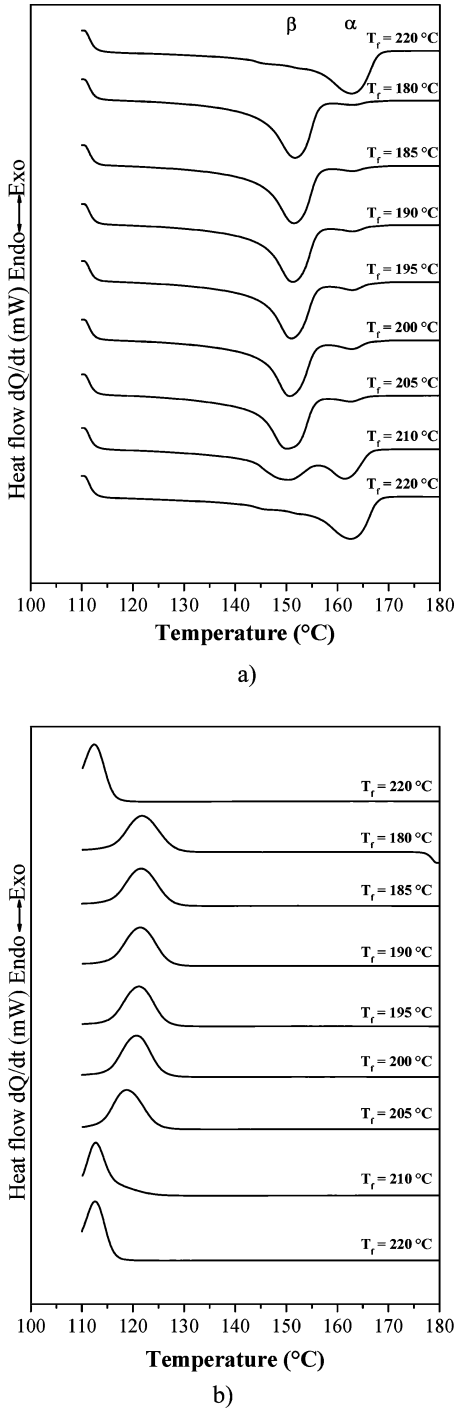

Figure 11. Effect of the final temperature of heating on the characteristics of melting (a) and crystallization (b) traces (C = 100 ppm, $V_c = V_h$ = 10 °C/min).

parts with a high β-phase content is around 300 ppm can be explained by the fact that the temperature of the melt was relatively high (240 °C) in this case.[19] It is worth mentioning that the samples obtained with "critical" nucleator concentration possess highest toughness.[19,23] On the contrary, the toughness of "supercritically" nucleated samples is lower, in spite of its β-content, which basically influenced the impact strength,[2] which is higher. This apparent contradiction can be explained with the difference in crystal habit or size of NJS in the "critically" and "supercrytically" nucleated samples. Indeed, NJS seems to be totally dissolved in iPP melt in the "critical" concentration range and recrystallized from the melt in finely dispersed form (Figure 7), which induced a very uniform

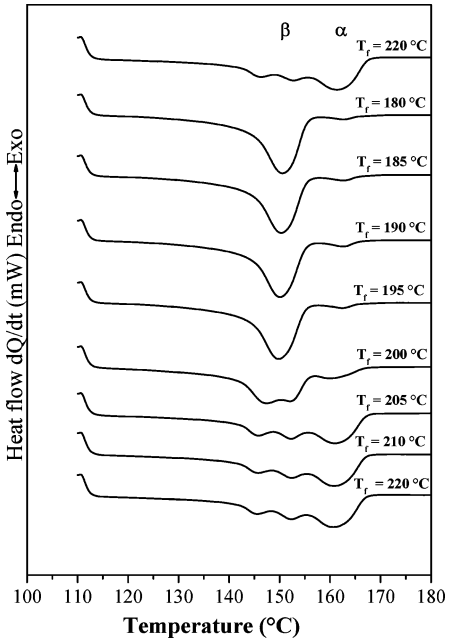

Figure 12. Effect of the final temperature of heating on the characteristics of melting traces ($C = 50$ ppm, $V_c = V_h = 10$ °C/min).

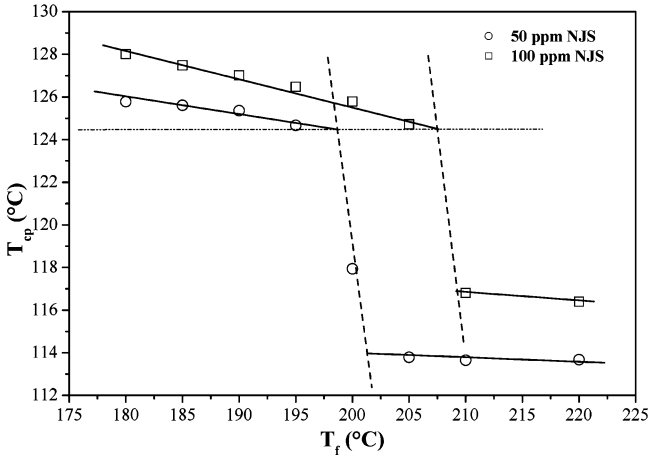

Figure 13. Peak temperature of crystallization (T_{cp}) characterizing the efficiency of the nucleating agent plotted against the final temperature of heating (T_f).

structure. In the "supercritically" nucleated samples, a part of introduced NJS remains in the primary form, leading to the formation of a rougher and inhomogeneous supermolecular structure, which is disadvantageous for toughness. Based on our experience, the results of Nezbedova et al.,[16] which showed that the fracture properties of compression-molded samples (T_f = 220 °C), were better after slow cooling than after quenching can be also explained easily. The thermal conditions for the recrystallization of the nucleating agent partially dissolved in the polymer are obviously more advantageous when the sample is cooled slowly than in the case of quenching, what leads to higher efficiency. This yields a higher β-content in compression-molded parts.

Conclusions

PLM and DSC studies showed the partial or complete dissolution and a dual (α and β) nucleating effect of NJS. The amount of not dissolved, heterogeneous nucleating agent content of the melt is determined by its initial concentration and by the final temperature of melting. These factors as well as the thermal conditions of cooling and crystallization strongly influence the

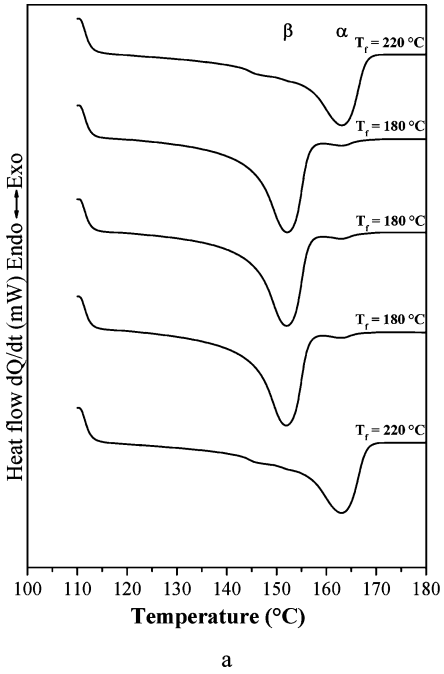

a

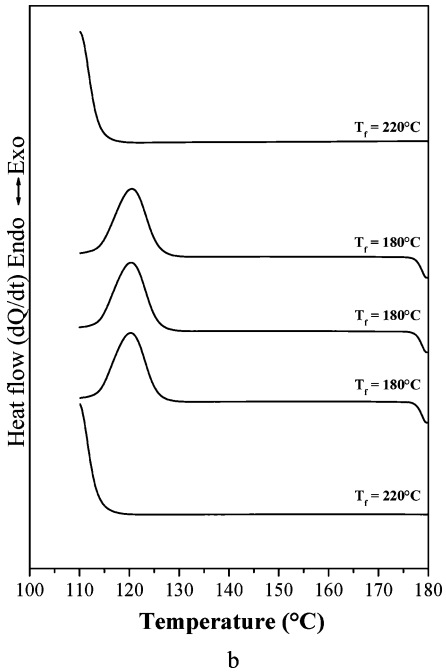

b

Figure 14. Melting (a) and crystallization (b) traces recorded on samples with different thermal history ($C = 100$ ppm, $V_c = V_h = 10$ °C/min).

crystallization process, the polymorphic composition, and the resulting supermolecular structure of the product. Dual nucleation results from the partial α-nucleating ability of the lateral surface of NJS needle crystals. The model proposed in this article explains fairly well both structure formation and the dual nucleation feature of NJS.

Acknowledgment. The authors are grateful to the Hungarian Research Foundation (OTKA T 49340) for supporting the research presented here.

References and Notes

(1) Varga, J. *J. Macromol. Sci., Phys.* **2002**, *B41*, 1121−1171.
(2) Grein, C. *Adv. Polym. Sci.* **2005**, *188*, 43−104.

(3) Turner Jones, A.; Aizlewood, J. M.; Beckett, D. R. *Macromol. Chem.* **1964**, *75*, 134−154.
(4) Menyhard, A.; Varga, J.; Molnar, G. *J. Therm. Anal. Calorim.* **2006**, *83*, 625−630.
(5) Leugering, H. *J. Macromol. Chem.* **1967**, *109*, 204−216.
(6) Shi, G.; Zhang, X.; Qiu, Z. *Macromol. Chem.* **1992**, *193*, 583−591.
(7) Varga, J.; Mudra, I.; Ehrenstein, G. W. *J. Appl. Polym. Sci.* **1999**, *74*, 2357−2368.
(8) Li, X.; Hu, K.; Li, M.; Huang, Y.; Zhou, G. *J. Appl. Polym. Sci.* **2002**, *86*, 633−638.
(9) Ikeda, N.; Kobayashi, T.; Killough, L. Polypropylene '96. World Congress, Zurich, Switzerland, Sept 18−20, 1996.
(10) Varma-Nair, M.; Agarwal, P. K. *J. Therm. Anal. Calorim.* **2000**, *59*, 483−495.
(11) Marco, C.; Gomez, M. A.; Ellis, G.; Arribas, J. M. *J. Appl. Polym. Sci.* **2002**, *86*, 531−539.
(12) Cho, K.; Saheb, D. N.; Choi, J.; Yang, H. *Polymer* **2002**, *43*, 1407−1416.
(13) Cho, K.; Saheb, D. N.; Yang, H. C.; Kang, B. I.; Kim, J.; Lee, S. S. *Polymer* **2003**, *44*, 4053−4059.
(14) Obadal, M.; Cermak, R.; Cabla, R.; Stoklasa, K. *Antek* **2004**, 3043−3049.
(15) Romankiewicz, A.; Sterzynski, T.; Brostow, W. *Polym. Int.* **2004**, *53*, 2086−2091.
(16) Nezbedova, E.; Pospisil, V.; Bohaty, P.; Vlach, B. *Macromol. Symp.* **2001**, *170*, 349−357.
(17) Bohaty, P.; Vlach, B.; Seidler, S.; Koch, T.; Nezbedova, E. *J. Macromol. Sci., Phys.* **2002**, *B41*, 657−669.
(18) Romankiewicz, A.; Sterzynski, T. *Macromol. Symp.* **2002**, *180*, 241−256.
(19) Kotek, J.; Raab, M.; Baldrian, J.; Grellmann, W. *J. Appl. Polym. Sci.* **2002**, *85*, 1174−1184.
(20) Scudla, J.; Raab, M.; Eichhorn, K. J.; Strachota, A. *Polymer* **2003**, *44*, 4655−4664.
(21) Kotek, J.; Kelnar, I.; Baldrian, J.; Raab, M. *Eur. Polym. J.* **2004**, *40*, 679−684.
(22) Obadal, M.; Cermák, R.; Stoklasa, K.; Petruchová, M. *Antek* **2003**, 1479−1483.
(23) Obadal, M.; Cermak, R.; Baran, N.; Stoklasa, K.; Simonik, J. *Int. Polym. Process.* **2004**, *19*, 35−39.
(24) Obadal, M.; Cermak, R.; Habrova, V.; Stoklasa, K.; Simonik, J. *Int. Polym. Process.* **2004**, *19*, 308−312.
(25) Cermak, R.; Obadal, M.; Ponizil, P.; Polaskova, M.; Stoklasa, K.; Lengalova, A. *Eur. Polym. J.* **2005**, *41*, 1838−1845.
(26) Cermak, R.; Obadal, M.; Ponizil, P.; Polaskova, M.; Stoklasa, K.; Heckova, J. *Eur. Polym. J.* **2006**, *42*, 2185−2191.
(27) Zhou, J.-J.; Liu, J.-G.; Yan, S.-K.; Dong, J.-Y.; Li, L.; Chan, C.-M.; Schultz, J. M. *Polymer* **2005**, *46*, 4077−4087.
(28) Hou, W. M.; Liu, G.; Zhou, J. J.; Gao, X.; Li, Y.; Li, L.; Zheng, S.; Xin, Z.; Zhao, L. Q. *Colloid Polym. Sci.* **2006**, *285*, 11−17.
(29) Behrendt, N.; Mohmeyer, N.; Hillenbrand, J.; Klaiber, M.; Zhang, X. Q.; Sessler, G. M.; Schmidt, H. W.; Altstadt, V. *J. Appl. Polym. Sci.* **2006**, *99*, 650−658.
(30) Olley, R. H.; Bassett, D. C. *Polymer* **1982**, *23*, 1707−1710.
(31) Varga, J. *J. Mater. Sci.* **1992**, *27*, 2557−2579.
(32) Varga, J. *Angew. Makromol. Chem.* **1983**, *112*, 191−203.
(33) Varga, J. In *Polypropylene: Structure, Blends and Composites*; Karger-Kocsis, J., Ed.; Chapman & Hall: London, 1995; Vol. 1, pp 56−115.
(34) Samuels, R. J. *J. Polym. Sci., Part B: Polym. Phys.* **1975**, *13*, 1417−1446.
(35) Vychopnova, J.; Habrova, V.; Obadal, M.; Cermak, R.; Cabla, R. *J. Therm. Anal. Calorim.* **2006**, *86*, 687−691.
(36) Varga, J.; Ehrenstein, G. W. *Colloid Polym. Sci.* **1997**, *275*, 511−519.
(37) Trifonova-Van Haeringen, D.; Varga, J.; Ehrenstein, G. W.; Vancso, G. J. *J. Polym. Sci., Part B: Polym. Phys.* **2000**, *38*, 672−681.
(38) Varga, J.; Schulek-Toth, F.; Ille, A. *Colloid Polym. Sci.* **1991**, *269*, 655−664.

MA062815J